Journal of Geoscience and Environment Protection, 2026, 14(1), 337-353
https://www.scirp.org/journal/gep
ISSN Online: 2327-4344
ISSN Print: 2327-4336

Geochemical Features of Alkaline Lavas from Nkondjock (Littoral-Cameroon): Geodynamic Implication

Synthia Nguimatsia Tengomo[1*], Paterne Mulimbi Kagarabi[1,2], Rodolph Loïque Azefack Mbounou[1], Sylvin Sans-Terres Tedonkenfack[1], David Guimolaire Nkouathio[1]

[1]Department of Earth Sciences, Faculty of Sciences, University of Dchang, Dschang, Cameroun
[2]Filière de Géologie, Domaine de Sciences et Technologie, Université Officielle de Bukavu, Bukavu, RDC
Email: *nguimatsia7026@gmail.com

How to cite this paper: Tengomo, S. N., Kagarabi, P. M., Mbounou, R. L. A., Tedonkenfack, S. S.-T., & Nkouathio, D. G. (2026). Geochemical Features of Alkaline Lavas from Nkondjock (Littoral-Cameroon): Geodynamic Implication. *Journal of Geoscience and Environment Protection, 14,* 337-353.
https://doi.org/10.4236/gep.2026.141018

Received: December 16, 2025
Accepted: January 24, 2026
Published: January 27, 2026

Abstract

This study presents a comprehensive geochemical analysis of alkaline lavas from the Nkondjock area along the Cameroon Volcanic Line (CVL). Employing thin-section microscopy, ICP-AES (major elements), and ICP-MS (trace/REE elements), we characterize basanites (plagioclase, olivine, augite, opaque minerals and accessory spinel), hawaiites (plagioclase, olivine, augite and opaque minerals), mugearites (plagioclase, augite, aegirine, hornblende, opaque minerals and olivine), and benmoreites (plagioclase, augite, nepheline, sanidine, opaque minerals and accessory olivine). These lavas exhibit microlitic to porphyritic textures, indicating multi-stage crystallization: initial megacryst formation in magma chambers, phenocryst development in conduits, and rapid surface cooling. Geochemically, they are MgO-depleted (2.13 - 9.01 wt%) and Al_2O_3-enriched, with primitive mantle-normalized patterns showing LILE/LREE enrichment and OIB-like signatures. Crustal contamination is negligible, except in evolved samples (mugearite, benmoreite). Trace element ratios (e.g., La/Ta = 14.91 - 21.5; ΔNb > 0) confirm an asthenospheric garnet-lherzolite source, with low-degree partial melting (0.5% - 2%) at 70 - 80 km depth. Zr/Y (9.28 - 16.53) and Ti/Y (260 - 827) ratios classify them as intraplate basalts, consistent with reactivated Pan-African fault magmatism.

Keywords

Alkaline Lavas, Nkondjock, Cameroon Volcanic Line, OIB-Like Signatures, Asthenospheric Garnet-Lherzolite Source

1. Introduction

The Cameroon Volcanic Line (CVL), a major tectono-magmatic mega-structure trending N30˚E, extends over 1600 km in length and ~100 km in width (Tchoua, 1974; Njome & De Wit, 2014). Comprising both oceanic and continental segments, it represents a globally unique feature in Africa and worldwide (Déruelle et al., 1991, 2007). The oceanic sector (Atlantic) includes four volcanic islands, Pagalù, São Tomé, Príncipe, and Bioko, aligned within the Gulf of Guinea, along with two large seamounts between Bioko-Príncipe and Príncipe-São Tomé (Burke, 2001). The continental sector spans from Mount Cameroon to Lake Chad and hosts multiple volcanic edifices ranging in age from the Eocene to Recent (Fitton, 1987; Itiga et al., 2004). Mafic and felsic lavas occur across all CVL centers: Mounts Cameroon, Manengouba, Bambouto, Bamenda, and Mandara (Aka et al., 2004, 2018), except Mount Etindé, which consists exclusively of nephelinites, leucitites, and haüynophyres (Nkoumbou et al., 1995). While tectonically active since the Precambrian, magmatism only initiated at the end of the Cretaceous with the emplacement of ring complexes (Fosso et al., 2005).

The CVL's origin remains debated within the global scientific community, particularly in Cameroon. Some authors attribute it to the reactivation of Precambrian faults driving rifting (Fitton, 1980; Moreau et al., 1994), while others invoke a mantle thermal anomaly ("hot spot") (Meyers et al., 1998; Déruelle et al., 2007). Marzoli et al. (1999) contested Fitton's unified hot-spot model (Fitton & Dunlop, 1985; Fitton, 1987) using $^{40}Ar/^{39}Ar$ dating. Despite extensive research, the Nkondjock locality, underlain by significant volcanic formations, remains unexplored along the CVL. This article presents novel geochemical data from Nkondjock (Lat. 4˚40' - 5˚01'N, Long. 10˚08' - 10˚24'E; **Figure 1**), situated between Mount Bana and the Noun Plain. Underlain by Pan-African granites/gneisses (Kamguia Kamani et al., 2021; Azefack Mbounou et al., 2023), the area exposes mafic-intermediate volcanic rocks but lacks felsic types (Tengomo et al., 2026). By analyzing these samples, we constrain magma sources and evolution processes, directly addressing the CVL's disputed origin and refining regional tectonic-petrogenetic models.

2. Methods

Following field sampling, laboratory analyses comprised thin section preparation, microscopic description, and whole-rock geochemical analyses. Thin sections were prepared using standard protocols and examined under a polarizing microscope. Observations in both plane-polarized and cross-polarized light enabled the identification of mineral assemblages, textures, parageneses, and deformation microstructures based on classical optical criteria.

Whole-rock geochemical analyses targeted major elements, trace elements, and rare earth elements (REEs). Selected samples were powdered after removal of altered portions, controlled crushing, and milling. Major elements were analyzed by Inductively Coupled Plasma Atomic Emission Spectrometry (ICP-AES), while

trace elements and REEs were determined via Inductively Coupled Plasma Mass Spectrometry (ICP-MS) following lithium borate fusion. Major element concentrations are expressed as weight percent oxides; trace elements and REEs are reported in parts per million (ppm). Loss on ignition (LOI) was determined by calcination at 1000˚C to assess volatile content and the degree of sample alteration.

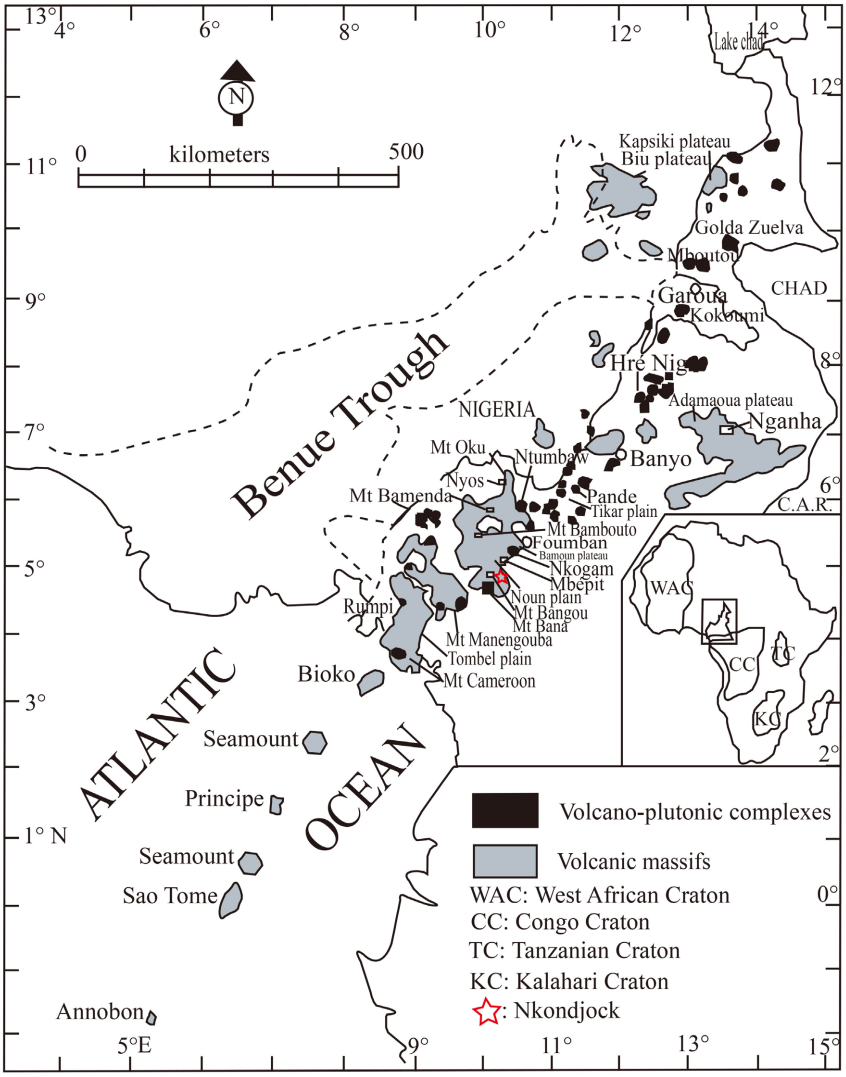

Figure 1. Location of the Nkondjock area (red star) along the Cameroon volcanic line (base map is from Njonfang et al., 2011). Locations of seamounts according to Burke (2001).

3. Results

3.1. Rock Classification

Volatile-free normalized major element compositions were used for classification. Preliminary analysis of Nkonjock volcanic rocks on a total alkalis vs. silica diagram (Le Bas et al., 1986) identifies mafic samples as alkaline, specifically comprising basanites, hawaiites, mugearites, and benmoreites (**Figure 2(a)**). This alkaline suite is further classified as potassic based on **Figure 2(b)**.

3.2. Petrography

The study reveals a diversity of alkaline lavas: basanites, hawaiites, mugearites, and benmoreites, representing distinct stages of magmatic differentiation within the study area. All these lavas generally exhibit microlitic textures (ranging from aphyric to fluidal variants, Figure 3(a)) and porphyritic textures (Figure 3(b)).

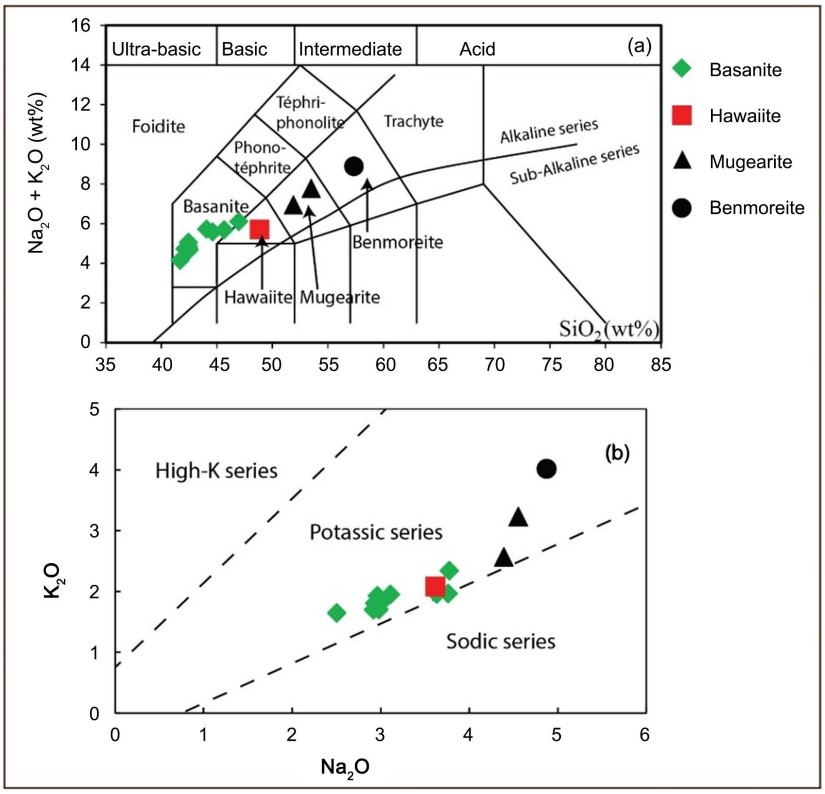

Figure 2. Classification of the Nkondjock lavas. (a) Position of the lavas on the TAS diagram of Le Bas et al. (1986). The bold line represents the Irvine-Barragar boundary (Irvine & Baragar, 1971) separating the alkaline series from the sub-alkaline series. (b) Position of the lavas on the Na_2O versus K_2O diagram of Le Maitre (2002).

3.2.1. Basanites

Basanites outcrop primarily as prismatic flows, domes, and stream-bed flows. Prismatic flows (often hexagonal) exhibit diameters of 10 - 30 cm. These rocks are mostly aphyric at the outcrop scale, occasionally semi-crystalline with visible olivine and pyroxene crystals.

In thin section, basanites display aphyric to porphyritic microlitic textures, sometimes fluidal. They comprise plagioclase (30% - 35%), olivine (15% - 20%), augite (10% - 15%), opaque minerals (5% - 10%), and accessory spinel. The mesostasis is cryptocrystalline, consisting of plagioclase microlites, olivine microcrystals, opaques, and volcanic glass. Olivines are frequently altered to iddingsite, while augites show well-developed cleavage and oblique extinction. Spinels occur as octahedral phenocrysts, occasionally surrounded by reaction rims (Figure 3(h)).

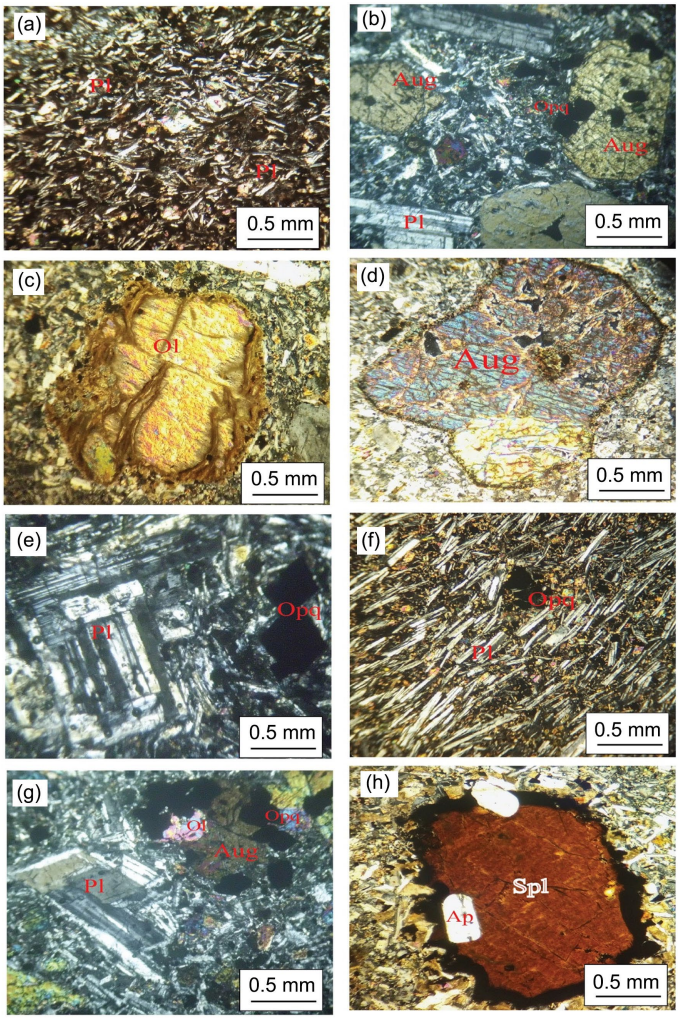

Figure 3. Microphotography of Nkondjock lavas. (a) Microlitic texture. (b) Porphyritic texture. (c) Olivine iddingsitization. (d) Augite crystal rimmed by opaques. (e) Zoned plagioclase. (f) Alignment of plagioclase microlites. (g) Opaque minerals as inclusions in plagioclase, augite, and olivine. (h) Spinel surrounded by reaction rim.

3.2.2. Hawaiites

Hawaiites form vegetation-covered domes. Macroscopically, they contain plagioclase and pyroxene phenocrysts. Thin sections reveal dominantly porphyritic microlitic textures with fluidal structure marked by the preferential alignment of plagioclase microlites (**Figure 3(f)**). Mineralogy is dominated by plagioclase (45% - 50%), followed by olivine (5% - 10%), augite (5% - 10%), and opaque minerals (1% - 5%). The cryptocrystalline mesostasis is rich in plagioclase microlites, olivine/augite microcrystals, opaques, and volcanic glass. Olivines locally exhibit iddingsitization (**Figure 3(c)**); augites are euhedral, non-pleochroic, and display moderate oblique extinction.

3.2.3. Mugearites

Mugearites outcrop as extensive domes (partly concealed by vegetation), locally showing incipient prismation. Samples exhibit a semi-crystalline structure.

Microscopically, they feature porphyritic to aphyric microlitic textures with pronounced fluidal structure. Composition includes plagioclase (40% - 45%), augite (10% - 15%), aegirine (2% - 5%), basaltic hornblende (~3%), opaque minerals (1% - 5%), and rare olivine (~2%). Zoned plagioclases dominate (Figure 3(e)), forming local glomeroporphyritic clusters. Augites are euhedral with high oblique extinction, often associated with opaques and aegirines. Opaque minerals are often found as inclusions in plagioclase, augite, and olivine (Figure 3(g)). The mesostasis is rich in plagioclase microlites, mafic microcrystals, and volcanic glass.

3.2.4. Benmoreites

Benmoreites occur as domes and isolated blocks. Macroscopically, they contain visible pyroxene crystals. Thin sections show a porphyritic microlitic texture. The mineralogy is dominated by plagioclase (~55%), with augite (10% - 15%), nepheline (1% - 5%), sanidine (1% - 3%), opaque minerals (1% - 5%), and accessory olivine (1% - 2%). Plagioclases appear as megacrysts to microlites, often corroded by mesostasis. Augites are euhedral with distinct oblique extinction, commonly rimmed by opaques (Figure 3(d)). The coexistence of sanidine and nepheline attests to the evolved alkaline character of these lavas.

3.3. Whole-Rock Major- and Trace-Element Geochemistry

Major- and trace-element compositions of the studied samples are presented in Table 1 and Table 2. The Nkonjock alkaline suite exhibits SiO_2 contents ranging from 39.6 to 56 wt% and MgO from 9.01 to 2.13 wt%. Benmoreite NJ45 has the highest SiO_2 and lowest MgO, whereas basanite NG60 shows the lowest SiO_2 and highest MgO (Figure 4). All basanites contain ≤45.8 wt% SiO_2, while mugearites range between 51 - 52.5 wt%.

Table 1. Whole-rock major element analysis and CIPW norms of Nkondjock lavas.

Rocks type	BASANITES											HAWAIITE	MUGEARITES		BENMOREITE
Samples	NA16	NL17	ND52	NK28	NS30	NS38	NT23	NK25	NG60	NE20	NK44	NS1	NM5	NO62	NJ45
SiO_2	44.9	43.8	42.7	41	40.8	41.6	40.1	45.8	39.6	40.8	41.1	46.3	51.4	52.5	56
TiO_2	2.94	3.53	3.4	4.2	4.09	4.18	4.04	2.84	2.9	4.06	4.14	2.46	1.99	1.75	1.42
Al_2O_3	15.55	16.05	16	14.9	15.1	15.25	14.85	15.7	13.45	15	15.2	15.45	18.1	16.25	16.25
Fe_2O_3	14.95	14.3	14.65	15.1	14.85	15.1	14.65	14.1	13.65	14.95	15.35	11.55	9.65	9.45	7.78
MnO	0.25	0.23	0.23	0.2	0.19	0.2	0.2	0.26	0.21	0.21	0.2	0.21	0.2	0.2	0.28
MgO	5.03	5.01	4.41	7.2	6.98	6.97	6.75	4.19	9.01	7.02	6.93	4.83	2.96	3.9	2.13
CaO	7.99	9.9	7.68	8.6	8.96	8.97	8.54	7.41	11.4	8.64	9.21	7.8	7.1	5.92	4.68
Na_2O	3.57	3.74	3.48	2.89	2.81	3.05	2.8	3.68	2.38	2.86	2.86	3.43	4.35	4.47	4.76
K_2O	2.03	1.95	1.87	1.73	1.63	1.91	1.82	2.28	1.56	1.63	1.76	1.97	2.54	3.17	3.92
P_2O_5	1.16	0.87	1.28	0.79	0.81	0.8	0.79	1.24	0.84	0.81	0.82	0.75	0.77	0.54	0.43
LOI	2.37	1.14	2.89	1.5	2.16	1.46	3.03	2.17	2.64	1.96	1.71	3.78	2.12	1.31	2.38
Total	100.74	100.52	98.59	98.11	98.38	99.49	97.57	99.67	97.64	97.94	99.28	98.53	101.18	99.46	100.03
Mg#	43.07	44.06	40.36	51.74	51.38	50.93	50.88	40.05	59.74	51.36	50.37	48.46	40.82	48.13	38.10

Continued

CIPW NORMS															
Orthose	12.36	11.74	11.71	10.73	10.15	11.67	11.53	14.00	9.83	10.18	10.81	12.42	15.28	19.25	23.89
Albite	22.49	12.48	22.71	12.55	12.31	10.61	11.52	26.64	0.11	13.24	10.45	28.88	36.35	36.66	41.54
Anorthite	21.03	21.65	23.85	23.69	25.05	23.04	24.21	20.35	22.82	24.59	24.36	22.34	22.77	15.32	11.75
Nepheline	4.68	10.71	4.59	7.10	6.90	8.71	7.52	3.09	11.57	6.68	7.96	1.13	0.61	1.19	-
Diopside	10.66	19.26	7.13	13.30	13.77	14.88	13.34	8.60	26.25	12.86	14.90	11.78	7.10	9.61	8.06
Hypersthene	-	-	-	-	-	-	-	-	-	-	-	-	-	-	7.29
Olivine	17.76	12.87	17.53	19.70	19.08	18.38	19.08	16.38	19.08	19.72	18.73	14.59	10.63	11.66	2.33
Magnetite	2.66	2.51	2.68	2.73	2.70	2.69	2.71	2.53	2.51	2.72	2.75	2.12	1.69	1.67	1.38
Ilmenite	5.75	6.83	6.84	8.37	8.18	8.21	8.23	5.60	5.87	8.15	8.17	4.98	3.85	3.42	2.78
Apatite	2.61	1.94	2.96	1.81	1.87	1.81	1.85	2.82	1.96	1.87	1.86	1.75	1.71	1.21	0.97
TOTAL	100.00	100.00	100.00	100.00	100.00	100.00	100.00	100.00	100.00	100.00	100.00	100.00	100.00	100.00	100.00

Table 2. Whole-rock trace element and REE analysis of Nkondjock lavas.

Rocks type	**BASANITES**											**HAWAIITE**	**MUGEARITES**		**BENMOREITE**
Samples	NA16	NL17	ND52	NK28	NS30	NS38	NT23	NK25	NG60	NE20	NK44	NS1	NM5	NO62	NJ45
Cs	0.83	0.48	0.45	0.39	0.41	0.36	0.48	0.84	0.62	0.43	0.33	0.68	0.83	0.27	0.22
Rb	51.6	45.8	45.5	37.7	37.4	41.4	44.5	74.7	52.5	36.7	37.4	49.3	61.2	58.3	71
Ba	661	630	622	586	550	580	576	654	663	637	595	749	946	1025	1115
Th	6.82	6.46	6.14	6.24	5.75	6.3	6.03	7.98	7.62	5.77	6.29	6.31	8.13	7.77	9.62
U	1.93	1.8	1.8	1.75	1.62	1.71	1.79	2.12	1.88	1.74	1.76	1.55	2.08	1.88	2.39
Zr	392	337	397	355	330	358	340	459	284	342	360	309	408	456	554
Hf	8.8	7.53	9.25	8.09	7.22	8.04	7.73	9.85	6.13	7.95	7.83	7.57	8.76	10.05	11.4
Ta	4.8	4.9	4.7	4.1	3.4	4.2	3.6	4.4	3.2	4	3.7	3.4	5.1	4.6	4.8
Y	35.2	34.3	38.2	33.1	30.8	33.8	31.4	35.1	30.6	32	32.6	32.6	31.2	34	33.5
Nb	97.6	99	94.9	91.6	85.4	93.7	89	108.5	92.9	88.3	93	69.2	87.5	75.3	79.4
Cr	33	17	17	29	43	31	47	11	297	84	37	83	19	107	102
V	145	241	169	302	287	305	292	136	279	288	299	186	126	124	101
W	1	0.9	0.8	1.2	1.1	1	1.2	1.4	0.9	1.1	1.7	0.6	0.6	1	1.8
Ga	20.4	22.2	22.2	21.5	20.6	21.7	21.1	23	20.3	21	21.6	20.3	21.8	22.8	23.5
Sr	1350	964	1210	1220	1065	1030	1170	1315	933	1170	1065	804	969	520	422
Sn	2.2	1.8	1.7	2	1.7	1.9	1.8	2.4	1.7	1.9	1.9	1	2.2	1.4	1.7
La	74.3	73.1	71.9	65.2	62.1	66.3	64.9	78.9	68.8	63.8	66.6	61.7	68.2	82.4	92.1
Ce	147.5	138.5	145.5	128.5	122.5	130	126	156	127	125.5	131.5	117	129.5	152	163
Pr	17.55	16.2	18.4	15.45	14.7	15.9	15.3	19.2	14.85	15.15	16	14.25	15.7	17.4	17.25
Nd	67.6	58.1	72	59.2	55.7	59.7	57.5	76.9	59.2	57.5	61.1	52.2	59.1	61.5	59.9
Sm	12	10.8	13.15	11.7	10.5	11.7	11.15	13	10.2	10.85	11.45	10	9.77	10.85	10.05
Eu	3.54	3.21	4.02	3.49	2.95	3.32	3.34	4.34	3.3	3.15	3.26	2.67	3.21	2.63	2.48
Gd	10.95	9.68	11.5	9.99	9.27	9.93	9.73	11.3	9.33	9.58	10.2	8.41	8.09	8.52	7.58
Tb	1.44	1.39	1.64	1.34	1.36	1.44	1.35	1.44	1.31	1.34	1.35	1.29	1.16	1.34	1.24
Dy	7.2	7.13	7.99	7.08	6.56	6.94	6.96	7.58	6.63	6.82	6.96	6.68	6.49	6.75	6.41
Ho	1.33	1.34	1.5	1.36	1.22	1.24	1.26	1.46	1.3	1.32	1.34	1.26	1.22	1.3	1.21
Er	3.56	3.49	3.85	3.28	3.08	3.25	3.2	3.4	2.98	3.28	3.27	3.46	3.27	3.48	3.48
Tm	0.45	0.44	0.48	0.41	0.4	0.44	0.42	0.46	0.31	0.43	0.41	0.46	0.41	0.53	0.48
Yb	2.86	2.48	3.04	2.5	2.42	2.49	2.52	2.9	2.67	2.56	2.55	2.82	2.96	3.2	3.27
Lu	0.45	0.44	0.46	0.39	0.42	0.4	0.35	0.45	0.33	0.37	0.36	0.45	0.39	0.51	0.48
ΔNb	0.17	0.3	0.18	0.2	0.21	0.21	0.21	0.09	0.36	0.21	0.19	0.19	0.04	-0.08	-0.22

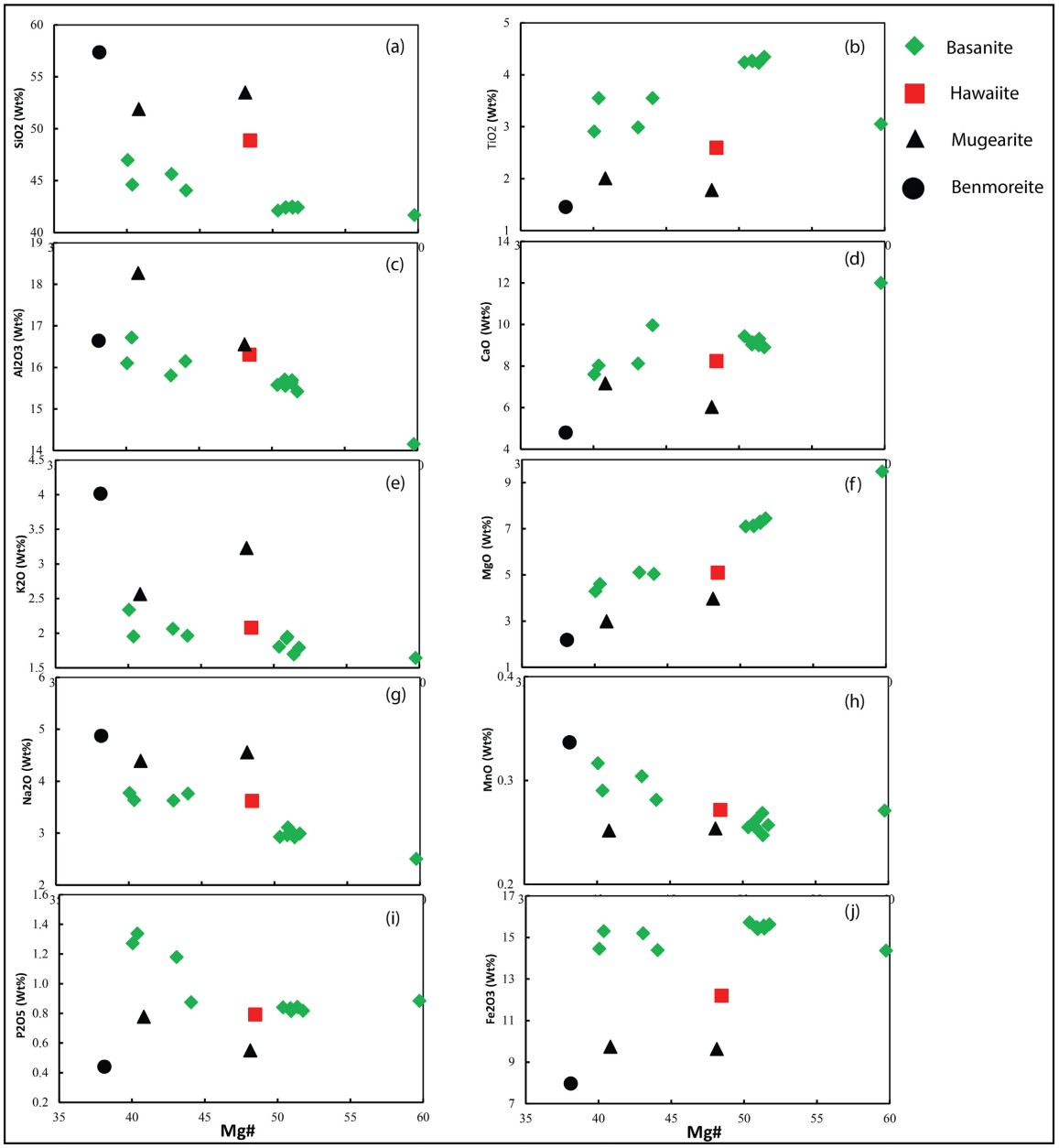

Figure 4. Major element variations for Nkondjock lavas against their Mg#.

Compared to lavas from the Cameroon Volcanic Line (CVL; Kagou et al., 2010; Tchuimegnie Ngongang et al., 2014; Mulimbi Kagarabi et al., 2025), Nkonjock lavas are depleted in MgO, enriched in Al_2O_3, and comparable in SiO_2, Na_2O, and K_2O. Normative mineralogy reveals nepheline in some samples and ubiquitous olivine, with hypersthene present only in benmoreite.

Primitive mantle-normalized (Sun & McDonough, 1989) trace element spider diagrams and REE patterns indicate enrichment in LILEs and LREEs relative to HFSEs and HREEs (**Figure 5**). This is evidenced by high (La/Yb) ratios: basanites (16.96 - 21.14), hawaiite (15.69), mugearites (16.52 - 18.47), and benmoreite (20.20). Patterns are parallel to Ocean Island Basalts (OIBs; **Figure 5**). Most sam-

ples exhibit slight positive Ba, Nb, La, and Zr anomalies, significant K and Ti anomalies (Figure 6(b)), and no Eu anomaly.

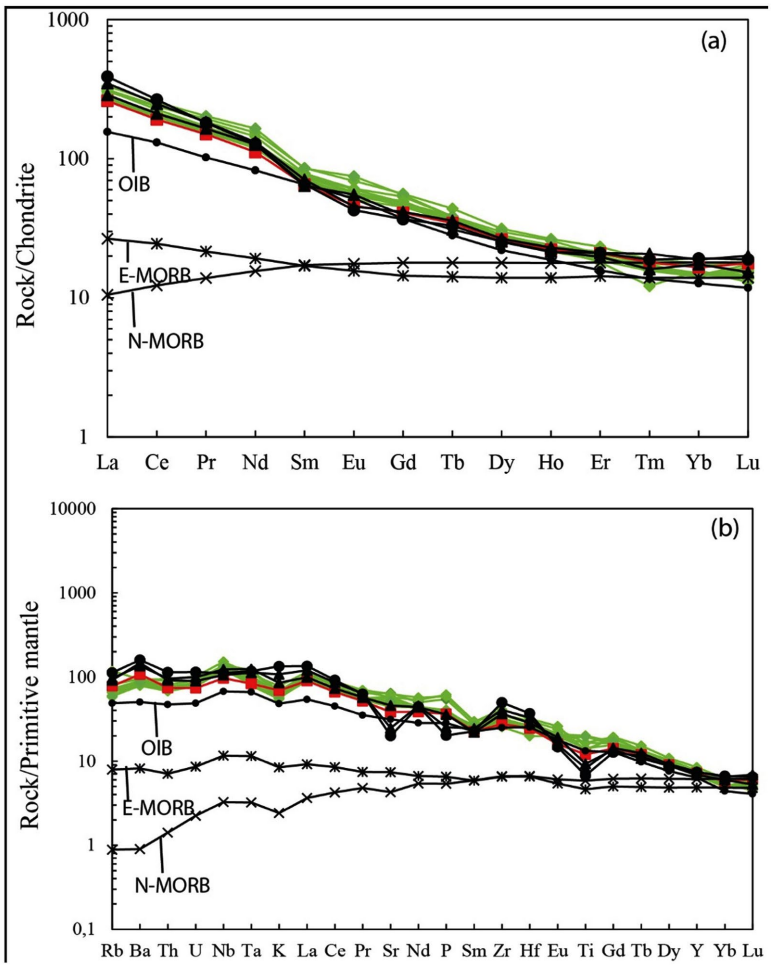

Figure 5. (a) Chondrite and (b) Primitive Mantle normalized spider diagrams of the Nkondjock lavas; normalization values are from Sun and McDonough (1989).

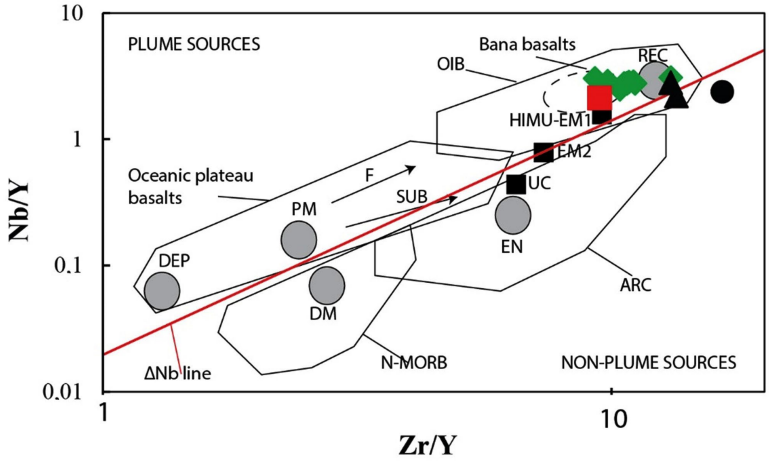

Figure 6. Studied lavas in the Zr/Y vs. Nb/Y diagram, relative to the mantle compositional components (circles) and fields of rocks from different tectonic settings after Condie, 2005.

4. Discussion

4.1. Petrography

The studied rocks generally exhibit microlitic textures (ranging from aphyric to fluidal variants) and porphyritic textures, with some samples containing plagioclase megacrysts. This suggests three distinct crystallization phases: formation of plagioclase megacrysts and opaque minerals in the magma chamber, development of phenocrysts/microphenocrysts of plagioclase, augite, olivine, and aegirine in the volcanic conduit, and rapid surface cooling leading to mesostasis formation. Corrosion embayments or growth gaps in plagioclase and olivine phenocrysts likely resulted from late-stage crystallization in residual melt during magma ascent. Opaque mineral rims around augite crystals (**Figure 3(d)**) indicate thermodynamic disequilibrium, attributed to rapid cooling or magmatic fluctuations. Plagioclase crystals preserve extensive magmatic histories; chemical zoning and mineral inclusions (**Figure 3(e)**) reflect evolving host-magma chemistry during growth, linked to shifting crystallization conditions. Normal zoning (anorthitic cores → albitic rims; Lindsey, 1966) implies constant-pressure cooling. Plagioclase alignment (**Figure 3(f)**) may indicate surface lava flow direction. Inclusions of opaque minerals and olivine in augite and ubiquitous opaque inclusions in plagioclase, olivine, and augite (**Figure 3(g)**) support fractional crystallization. Spinel phenocrysts (**Figure 3(h)**) suggest a mantle source. The textures and mineralogy reveal a multi-stage cooling history, emphasizing fractional crystallization and disequilibrium conditions. The absence of quartz/hypersthene (except in benmoreite) and spinel-olivine associations points to mantle-derived melts with limited shallow-crust interaction.

4.2. Petrogenesis

Provenance analysis for Nkondjock lavas considers ΔNb values: Mantle-derived lavas typically have ΔNb > 0. Here, ΔNb = 0.04 - 0.36 (**Table 2**), except for mugearite NO62 and benmoreite NJ45 (ΔNb = −0.07 and −0.22). In Nb/Y vs. Zr/Y plots (Weaver, 1991; Condie, 2005; **Figure 6**), most samples cluster in the mantle array (above ΔNb = 0), while NO62 and NJ45 plot below, indicating divergent behavior attributed to mantle source heterogeneities.

Vanadium (V) decreases systematically from basanites to benmoreites, confirming fractional crystallization as the primary differentiation mechanism. Steady Na_2O enrichment (**Figure 4(g)**) rules out significant plagioclase fractionation; instead, olivine, clinopyroxene, and Fe-Ti oxides dominated. Similar trends occur in Bafang, Fotouni, and Noun basalts. Uniform Nb/Th, Nb/Y, Zr/Nb, and Zr/Y ratios, consistent across the Cameroon Volcanic Line (CVL; e.g., Fitton, 1987; Kamgang et al., 2008), support a mantle origin.

4.3. Mantle Source Characteristics and Partial Melting

La/Ta ratios distinguish asthenospheric (≤22) from lithospheric (22 - 30) or contaminated (>30) sources. Nkondjock lavas yield La/Ta = 14.91 - 21.5, favoring an

asthenospheric origin. Ce/Yb vs. La/Ta plots (Figure 7) further indicate a garnet-bearing asthenospheric mantle. Trace elements show high La/Yb (21.87 - 29.47) and Zr/Y (9.85 - 16.53) with near-constant Y (30.8 - 35.2 ppm) and Yb (2.42 - 3.27 ppm), typifying garnet-dominated sources. Garnet stability (>3 GPa; ~70 - 80 km depth; Robinson & Wood, 1998) implies deep melting. Ce/Y vs. Zr/Nb (Figure 8) and La/Yb vs. Zr/Nb (Figure 9) diagrams align samples with primitive garnet peridotite (GP), suggesting 0.5% - 2% partial melting of garnet lherzolite (2% - 4% garnet), consistent with Bafang, Fotouni, Mt. Cameroon, and Manengouba lavas.

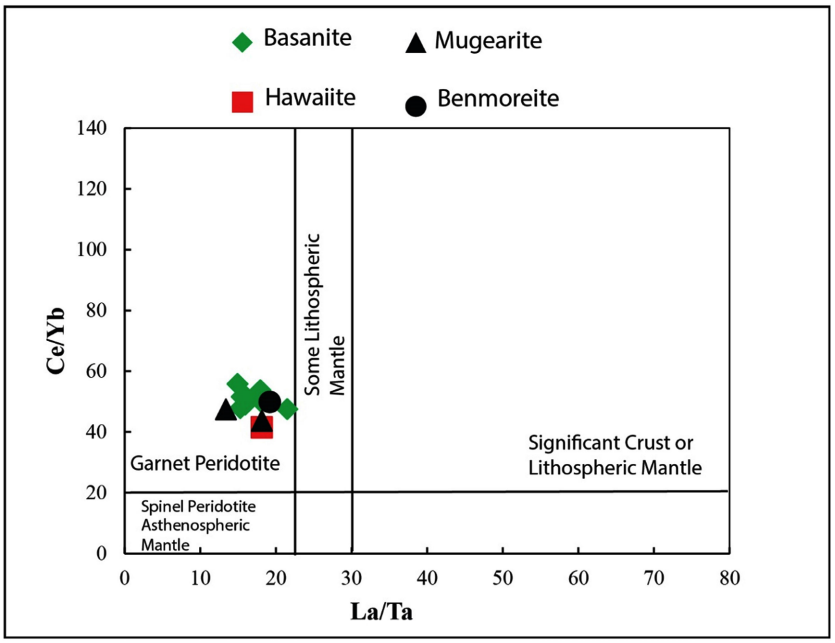

Figure 7. Ce/Yb vs. La/Ta for the source of the Nkondjock lavas after Dorais, Marvinney, and Markert (2017).

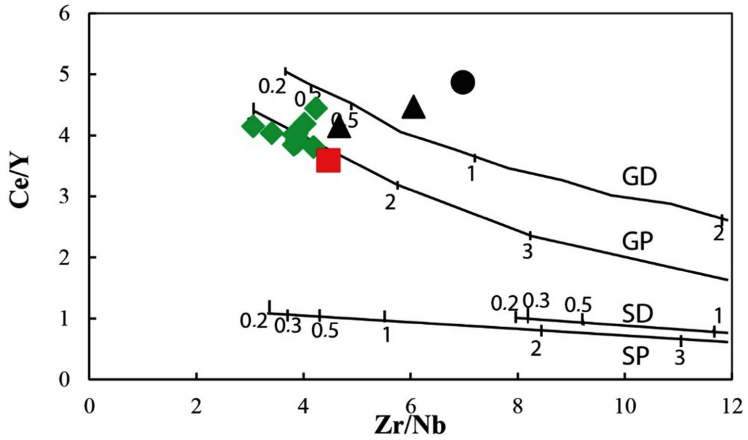

Figure 8. Ce/Y vs. Zr/Nb for the source of the Nkondjock lavas after de Hardarson and Fitton (1991). The bold curves represent non-modal fractional melting for four mantle compositions: GD: depleted garnet lherzolite; GP: primitive garnet lherzolite; SD: depleted spinel lherzolite; SP: primitive spinel lherzolite. The numbers on the lines correspond to the melting percentages.

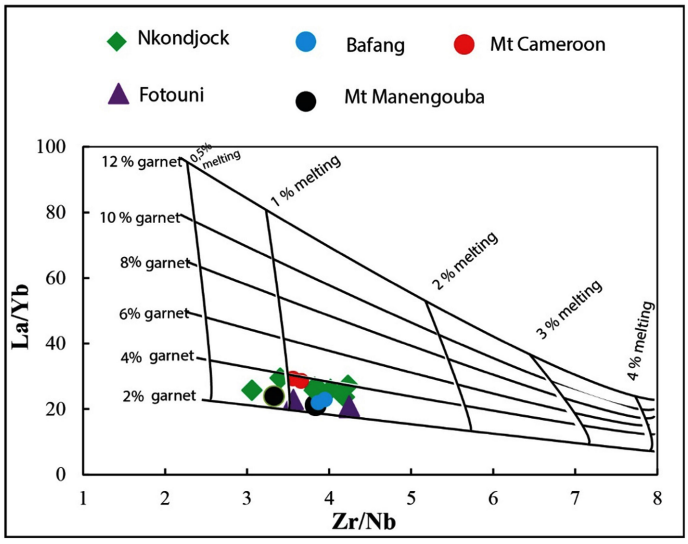

Figure 9. Modeled melting (Zr/Nb vs. La/Yb) result for the CVL mafic rocks with MgO > 4. Melts that produced most basanites and alkali basalts were generated by <3% partial melting of a dominantly garnet (<6%) bearing mantle lherzolite.

4.4. Crustal Contamination

Key contamination indicators (e.g., basement xenoliths, normative quartz/hypersthene) are absent, except in benmoreite. Elevated Ba (positive multi-element anomaly) hints at assimilation, but La/Nb (0.70 - 1.15) and La/Ta (13.37 - 21.5) contradict the criteria for crustal input (La/Nb > 1.5, La/Ta > 22; Hart et al., 1989). Negative Nb/Zr anomalies typical of contamination (Cai et al., 2010) are also lacking. Thus, crustal effects were negligible. This is confirmed by the Rb/Y vs. Nb/Y diagram (**Figure 10**) after Cox and Hawkesworth (1985). In this diagram, the studied lavas fall into the uncontaminated lava field.

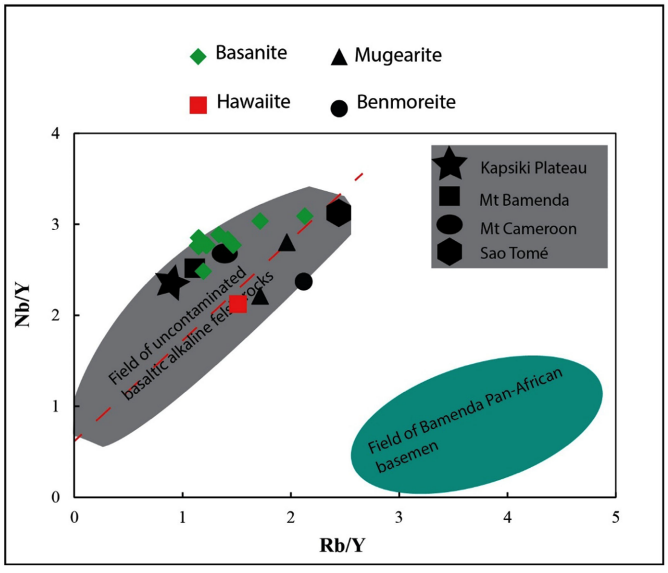

Figure 10. Nkondjock lavas in the Rb/Y vs. Nb/Y diagram after Cox and Hawkesworth (1985).

4.5. Geotectonic Context

Immobile elements (Ti, Y, Zr) constrain tectonic settings. High Ti/Y (260.23 - 827.36) and Zr/Y (9.28 - 16.53) ratios, coupled with positive Nb anomalies, characterize intraplate magmatism (Pearce & Cann, 1973). Zr/Ba ratios (0.41 - 0.70; Ormerod et al., 1988, 1991) exceed the subduction-related threshold (<0.2), confirming an intraplate affinity. Discrimination diagram (Zr/Y vs. Zr, **Figure 11**) consistently plots samples within within-plate basalt (WPB) fields. The high enrichment in incompatible elements (Rb, Ba, Nb, Th, and Zr), along with the REE spectra enriched in LREE, without marked Eu anomalies, indicates low-grade partial melting of an EM1 or EM2 enriched mantle, consistent with an OIB signature (Sun & McDonough, 1989). This context is reinforced by predominantly positive ΔNb values, thus ruling out a subduction environment (Pearce & Cann, 1973). Taken together, these data therefore suggest intraplate alkali volcanism.

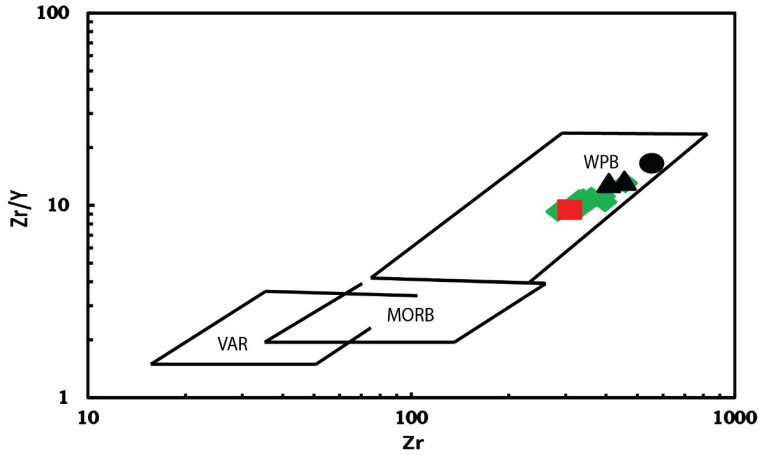

Figure 11. Nkondjock lavas in the tectonic evolution discriminant diagram Zr/Y vs. Zr after Pearce and Norry (1979). WPB = Intraplate Basalts, VAB = Volcanic Arc Basalts, MORB = Mid-Ocean Ridge Basalts.

This aligns with CVL models invoking intraplate alkaline magmatism along reactivated Pan-African faults (Njonfang et al., 2013).

5. Conclusion

The Nkondjock lavas originate from low-degree melting (0.5% - 2%) of garnet-bearing asthenospheric mantle at 70 - 80 km depth, fractionating via olivine, clinopyroxene, and Fe-Ti oxides during ascent. Their intraplate affinity; evidenced by high Zr/Y (9.28 - 16.53), positive Nb anomalies, and classification within within-plate basalt fields; provides robust support for the fault reactivation model over the mantle plume hypothesis for CVL genesis. This geochemical signature aligns unambiguously with magmatism driven by reactivated Pan-African structures, as indicated by:

- Trace element ratios (e.g., ΔNb > 0, La/Ta = 14.91 - 21.5) confirming asthenospheric sourcing without plume-like thermal anomalies.

- Tectonic discrimination (Zr/Y vs. Zr) excluding mantle plume affinities and instead correlating with rift-related fault systems. Petrographic textures further record disequilibrium crystallization during multi-stage ascent, while minimal crustal assimilation (La/Nb < 1.5) underscores mantle-dominated processes. Collectively, these findings position the CVL as a tectonically controlled rift province, with Nkondjock offering critical insights into deep melting dynamics at reactivated lithospheric discontinuities.

Conflicts of Interest

The authors declare no conflicts of interest regarding the publication of this paper.

References

Aka, F. T., Hasegawa, T., Nche, L. A., Asaah, A. N. E., Mimba, M. E., Teitchou, I. et al. (2018). Upper Triassic Mafic Dykes of Lake Nyos, Cameroon (West Africa) I: K-Ar Age Evidence within the Context of Cameroon Line Magmatism, and the Tectonic Significance. *Journal of African Earth Sciences, 141,* 49-59. https://doi.org/10.1016/j.jafrearsci.2018.02.001

Aka, F. T., Nagao, K., Kusakabe, M., Sumino, H., Tanyileke, G., Ateba, B. et al. (2004). Symmetrical Helium Isotope Distribution on the Cameroon Volcanic Line, West Africa. *Chemical Geology, 203,* 205-223. https://doi.org/10.1016/j.chemgeo.2003.10.003

Azefack Mbounou, R. L., Ganno, S., Ngnotue, T., Tanko Njiosseu, E. L., Fossi, D. H., Ngassam Mbianya, G. et al. (2023). Structural and Kinematic Analysis of the Nkondjock Shear Zone, Central Cameroon: Implications on the Geodynamic Evolution of the Central African Fold Belt. *Arabian Journal of Geosciences, 16,* Article No. 240. https://doi.org/10.1007/s12517-023-11336-x

Burke, K. (2001). Origin of the Cameroon Line of Volcano-Capped Swells. *The Journal of Geology, 109,* 349-362. https://doi.org/10.1086/319977

Cai, K., Sun, M., Yuan, C., Zhao, G., Xiao, W., Long, X., & Wu, F. (2010). Geochronological and Geochemical Study of Maic Dykes from the Northwest Chinese Altai: Implications for Petrogenesis and Tectonic Evolution. *Gondwana Research, 18,* 638-652. https://doi.org/10.1016/j.gr.2010.02.010

Condie, K. C. (2005). High Field Strength Element Ratios in Archean Basalts: A Window to Evolving Sources of Mantle Plumes? *Lithos, 79,* 491-504. https://doi.org/10.1016/j.lithos.2004.09.014

Cox, K. G., & Hawkesworth, C. J. (1985). Geochemical Stratigraphy of the Deccan Traps at Mahabaleshwar, Western Ghats, India, with Implications for Open System Magmatic Processes. *Journal of Petrology, 26,* 355-377. https://doi.org/10.1093/petrology/26.2.355

Déruelle, B., Moreau, C., Nkoumbou, C., Kambou, R., Lissom, J., Njonfang, E. et al. (1991). The Cameroon Line: A Review. In A. B. Kampunzu, & R. T. Lubala (Eds.), *Magmatism in Extensional Structural Settings* (pp. 274-327). Springer. https://doi.org/10.1007/978-3-642-73966-8_12

Déruelle, B., Ngounouno, I., & Demaiffe, D. (2007). The 'Cameroon Hot Line' (CHL): A Unique Example of Active Alkaline Intraplate Structure in Both Oceanic and Continental Lithospheres. *Comptes Rendus. Géoscience, 339,* 589-600. https://doi.org/10.1016/j.crte.2007.07.007

Dorais, M. J., Marvinney, R. G., & Markert, K. (2017). The Age, Petrogeneis and Tectonic

Significance of the Frontenac Formation Basalts, Northern New Hampshire and Western Maine. *American Journal of Science, 317,* 990-1018. https://doi.org/10.2475/09.2017.02

Fitton, J. G. (1980). The Benue Trough and Cameroon Line—A Migrating Rift System in West Africa. *Earth and Planetary Science Letters, 51,* 132-138. https://doi.org/10.1016/0012-821x(80)90261-7

Fitton, J. G. (1987). The Cameroon Line, West Africa: A Comparison between Oceanic and Continental Alkaline Volcanism. In J.G. Fitton, & B. G. J. Upton (Eds.), *Alka-Line Igneous Rocks* (pp. 273-291) Geological Society, London, Special Publications. https://doi.org/10.1144/gsl.sp.1987.030.01.13

Fitton, J. G., & Dunlop, H. M. (1985). The Cameroon Line, West Africa, and Its Bearing on the Origin of Oceanic and Continental Alkali Basalt. *Earth and Planetary Science Letters, 72,* 23-38. https://doi.org/10.1016/0012-821x(85)90114-1

Fosso, J., Ménard, J., Bardintzeff, J., Wandji, P., Tchoua, F. M., & Bellon, H. (2005). Les laves du mont Bangou: Une première manifestation volcanique éocène, à affinité transitionnelle, de la Ligne du Cameroun. *Comptes Rendus. Géoscience, 337,* 315-325. https://doi.org/10.1016/j.crte.2004.10.014

Hardarson, B. S., & Fitton, J. G. (1991). Increased Mantle Melting beneath Snaefellsjökull Volcano during Late Pleistocene Deglaciation. *Nature, 353,* 62-64. https://doi.org/10.1038/353062a0

Hart, W. K., WoldeGabriel, G., Walter, R. C. & Mertzman, S. A. (1989). Basaltic Volcanism in Ethiopia: Constraints on Continental Rifting and Mantle Interactions. *Journal of Geophysical Research, 94,* 7731-7748. https://doi.org/10.1029/JB094iB06p07731

Irvine, T.N. & Baragar, W.R.A. (1971). A Guide to the Chemical Classification of the Common Volcanic Rocks. *Canadian Journal of Earth Science, 8,* 523-548. https://doi.org/10.1139/e71-055

Itiga, Z., Chakam Tagheu, P. J., Wotchoko, P., Wandji, P., Bardintzeff, J. -M., & Bellon, H. (2004). La ligne du cameroun: Volcanologie et géochronologie de trois régions (Mont manengouba, plaine du noun et tchabal gangdaba). *Géochronique, 91,* 13-16.

Kagou Dongmo, A., Nkouathio, D., Pouclet, A., Bardintzeff, J., Wandji, P., Nono, A. et al. (2010). The Discovery of Late Quaternary Basalt on Mount Bambouto: Implications for Recent Widespread Volcanic Activity in the Southern Cameroon Line. *Journal of African Earth Sciences, 57,* 96-108. https://doi.org/10.1016/j.jafrearsci.2009.07.015

Kamgang, P., Chazot, G., Njonfang, E., & Tchoua, F. (2008). Geochemistry and Geochronology of Mafic Rocks from Bamenda Mountains (Cameroon): Source Composition and Crustal Contamination along the Cameroon Volcanic Line. *Comptes Rendus. Géoscience, 340,* 850-857. https://doi.org/10.1016/j.crte.2008.08.008

Kamguia Kamani, M. S., Wang, W., Tchouankoue, J. -P., Huang, S., Yomeun, B., Xue, E. et al. (2021). Neoproterozoic Syn-Collision Magmatism in the Nkondjock Region at the Northern Border of the Congo Craton in Cameroon: Geodynamic Implications for the Central African Orogenic Belt. *Precambrian Research, 353,* Article 106015. https://doi.org/10.1016/j.precamres.2020.106015

Le Bas, M. J., Le Maitre, R. W., Streickeisen, A., & Zanettin, B. (1986). A Chemical Classification of Volcanic Rocks Based on the Total Alkali-Silica Diagram. *Journal of Petrology, 27,* 745-750. https://doi.org/10.1093/petrology/27.3.745

Le Maitre, R. W. (2002). *Igneous Rock. A Classification and Glossary of Terms.* Cambridge University Press.

Marzoli, A., Renne, P. R., Piccirillo, E. M., Francesca, C., Bellieni, G., Melfi, A. J. et al.

(1999). Silicic Magmas from the Continental Cameroon Volcanic Line (Oku, Bambouto and Ngaoundere): 40 Ar-39 Ar Dates, Petrology, Sr-Nd-O Isotopes and Their Petrogenetic Significance. *Contributions to Mineralogy and Petrology, 135,* 133-150. https://doi.org/10.1007/s004100050502

Meyers, J. B., Rosendahl, B. R., Harrison, C. G. A., & Ding, Z. (1998). Deep-Imaging Seismic and Gravity Results from the Offshore Cameroon Volcanic Line, and Speculation of African Hotlines. *Tectonophysics, 284,* 31-63. https://doi.org/10.1016/s0040-1951(97)00173-x

Moreau, C., Demaiffe, D., Bellion, Y., & Boullier, A. -M. (1994). A Tectonic Model for the Location of Palaeozoic Ring Complexes in Aïr (Niger, West Africa). *Tectonophysics, 234,* 129-146. https://doi.org/10.1016/0040-1951(94)90208-9

Mulimbi Kagarabi, P., Chako-Tchamabe, B., Tamen, J., Tumba, K., & Nkouathio, D. G., et al. (2025). Mineralogical, Petrological, and Geochemical Features of Alkali Basalts from the Dibi Area, Adamawa Plateau (Cameroon Volcanic Line). *Journal of Geoscience and Environment Protection, 13,* 75-107. https://doi.org/10.4236/gep.2025.139005

Njome, M. S., & de Wit, M. J. (2014). The Cameroon Line: Analysis of an Intraplate Magmatic Province Transecting Both Oceanic and Continental Lithospheres: Constraints, Controversies and Models. *Earth-Science Reviews, 139,* 168-194. https://doi.org/10.1016/j.earscirev.2014.09.003

Njonfang, E., Nono, A., Kamgang, P., Ngako, V., & Tchoua, F. M. (2011). Cameroon Line alkaline magmatism (Central Africa): A reappraisal. *The Geological Society of America Special Paper, 478,* 173-191. https://doi.org/10.1130/2011.2478(09)

Njonfang, E., Tchoneng, G. T., Cozzupoli, D., & Lucci, F. (2013). Petrogenesis of the Sabongari Alkaline Complex, Cameroon Line (Central Africa): Preliminary Petrological and Geochemical Constraints. *Journal of African Earth Sciences, 83,* 25-54. https://doi.org/10.1016/j.jafrearsci.2013.03.004

Nkoumbou, C., Déruelle, B., & Velde, D. (1995). Petrology of Mt Etinde Nephelinite Series. *Journal of Petrology, 36,* 373-395. https://doi.org/10.1093/petrology/36.2.373

Pearce, J. A., & Cann, J. R. (1973). Tectonic Setting of Basic Volcanic Rocks Determined Using Trace Element Analyses. *Earth and Planetary Science Letters, 19,* 290-300. https://doi.org/10.1016/0012-821x(73)90129-5

Pearce, J. A., & Norry, M. J. (1979). Petrogenetic Implications of Ti, Zr, Y, and Nb Variations in Volcanic Rocks. *Contributions to Mineralogy and Petrology, 69,* 33-47. https://doi.org/10.1007/bf00375192

Robinson, J. A. C. & Wood, B. J. (1998). The Depth of the Garnet/Spinel Transition in Fractionally Melting Peridotite. *Earth and Planetary Science Letters, 164,* 277-284. https://doi.org/10.1016/S0012-821X(98)00213-1

Sun, S. -S., & McDonough, W. F. (1989). Chemical and Isotopic Systematics of Oceanic Basalts: Implications for Mantle Composition and Processes. In: A.D. Saunders, M. J. Norry (Eds.), *Magmatism in the Oceanic Basins* (Vol. 42, pp. 313-345). Geological Society, London, Special Publications. https://doi.org/10.1144/gsl.sp.1989.042.01.19

Tchoua, F. M. (1974). *Contribution à l'étude géologique et pétrographique de quelques volcans de la Ligne du Cameroun (Monts Manengouba et Bambouto)* (337 p). PhD Thesis, Université de Clermont-Ferrand.

Tchuimegnie Ngongang, N. B., Kamgang, P., Chazot, G., Agranier, A., Bellon, H., & Nonnotte, P. (2014). Age, Geochemical Characteristics and Petrogenesis of Cenozoic Intraplate Alkaline Volcanic Rocks in the Bafang Region, West Cameroon. *Journal of African Earth Sciences, 102,* 218-232. https://doi.org/10.1016/j.jafrearsci.2014.10.011

Tengomo, S. N., Azefack Mbounou, R. L., Kamgang Tchuifong, A. B., Pour, A. B., Nkouathio, D. V. (2026). Mapping Lithological Units and Alteration Minerals in Volcanic Rocks of Nkondjock, Littoral Region, Cameroon Using Sentinel-2 Remote Sensing Satellite Imagery and Comprehensive Fieldwork. *Journal of African Earth Sciences, 236,* 106003.

Weaver, B. L. (1991). The Origin of Ocean Island Basalt End-Member Compositions: Trace Element and Isotopic Constraints. *Earth and Planetary Science Letters, 104,* 381-397. https://doi.org/10.1016/0012-821x(91)90217-6